



# Intracranial substrates of meditation-induced neuromodulation in the amygdala and hippocampus

Christina Maher<sup>a,b</sup>, Lea Tortolero<sup>c</sup>, Soyeon Jun<sup>a,b</sup>, Daniel D. Cummins<sup>c</sup>, Adam Saad<sup>d</sup>, James Young<sup>d,e</sup>, Lizbeth Nunez Martinez<sup>a,b</sup>, Zachary Schulman<sup>c</sup>, Lara Marcuse<sup>d,e</sup>, Allison Waters<sup>a,b,e,f</sup>, Helen S. Mayberg<sup>a,b,c,d,e,f</sup>, Richard J. Davidson<sup>g</sup>, Fedor Panov<sup>c,e</sup>, and Ignacio Saez<sup>a,b,c,d,e,1</sup>

Edited by Michael Goldberg, Columbia University, New York, NY; received May 17, 2024; accepted December 2, 2024

Meditation is an accessible mental practice associated with emotional regulation and well-being. Loving-kindness meditation (LKM), a specific subtype of meditative practice, involves focusing one's attention on thoughts of well-being for oneself and others. Meditation has been proven to be beneficial in a variety of settings, including therapeutic applications, but the neural activity underlying meditative practices and their positive effects are not well understood. It has been difficult to understand the contribution of deep limbic structures given the difficulty of studying neural activity directly in the human brain. Here, we leverage a unique patient population, epilepsy patients chronically implanted with responsive neurostimulation devices that allow chronic, invasive electrophysiology recording to investigate the physiological correlates of LKM in the amygdala and hippocampus of novice meditators. We find that LKM-associated changes in physiological activity were specific to periodic, but not aperiodic, features of neural activity. LKM was associated with an increase in  $\gamma$  (30 to 55 Hz) power and an alternation in the duration of  $\beta$  (13 to 30 Hz) and  $\gamma$  oscillatory bursts in both the amygdala and hippocampus, two regions associated with mood disorders. These findings reveal the nature of LKM-induced modulation of limbic activity in first-time meditators.

loving-kindness meditation | amygdala | hippocampus | intracranial electrophysiology

Meditation is a set of mental techniques aimed at cultivating well-being, which require honing attentional skills related to emotional regulation (1–5). Numerous studies have proven that meditation can improve mental well-being in population-based settings (6), and potentially improve psychiatric diseases such as anxiety and depression (7). In concert with its clinical effects, meditation has been shown to change brain activity assessed through electrophysiology and functional neuroimaging (8, 9). Recent literature has parceled out primary categories of meditation, thus allowing rigorous scientific evaluation of specific practices (10). Loving-kindness meditation (LKM) is a technique within the constructive meditation family, in which practitioners actively focus their attention on cultivating positive thoughts of well-being for oneself and others. Preliminary work has suggested varying forms of meditation may share common effects on brain electrophysiology (11): This remains an important area for potential study. LKM may have therapeutic potential through the cultivation of positive emotion (12), but its underlying neural correlates are not well known, especially in deep brain areas involved in emotional regulation.

Functional and structural MRI studies have demonstrated changes in both the amygdala and the hippocampus from continued LKM practice (13, 14). EEG studies, in addition, have shown increased  $\gamma$  activity during meditation (11, 14), including during LKM in experienced meditators (3). BOLD-fMRI signals have been shown to correlate with  $\gamma$  activity (15), suggesting that these processes are related. Therefore, we first hypothesized that LKM is associated with increased  $\gamma$ -band power and duration of  $\gamma$ -band oscillatory events in both the amygdala and hippocampus (3, 11, 14). Regulation in other frequency bands may accompany gamma changes: FA meditation is linked to decreased long-range neuronal synchrony within and between brain regions.  $\beta$  oscillations are associated with attentional shifts in nonhuman and human primates: When animals are paying attention to external stimuli, beta coherence is increased to support effective information-gathering (16–19). During LKM, participants are turned to turn attention away from external stimuli and inward; therefore, we additionally hypothesized that LKM would be associated with decreased power or duration of  $\beta$  oscillatory events compared to baseline.

Despite this theoretical basis for our hypotheses regarding LKM-associated changes in neuronal activity several additional questions remain. For example, whether LKM is discretely associated with oscillatory processes rather than an overall excitation/inhibition profile

## Significance

We leverage rare chronic, invasive electrophysiology recordings while participants engage in loving-kindness meditation to demonstrate that meditation induces neural changes in beta and gamma activity in the amygdala and hippocampus of novice meditators. These results build on previous findings in experienced meditators and reveal meditation's potential for noninvasive neuromodulation of brain activity associated with emotional regulation and mood disorders.

Author affiliations: <sup>a</sup>Nash Family Department of Neuroscience, Icahn School of Medicine at Mount Sinai, New York, NY 10029; <sup>b</sup>The Friedman Brain Institute, Icahn School of Medicine at Mount Sinai, New York, NY 10029; <sup>c</sup>Department of Neurosurgery, Icahn School of Medicine at Mount Sinai, New York, NY 10029; <sup>d</sup>Department of Neurology, Icahn School of Medicine at Mount Sinai, New York, NY 10029; <sup>e</sup>Nash Family Center for Advanced Circuit Therapeutics, Icahn School of Medicine at Mount Sinai, New York, NY 10029; <sup>f</sup>Department of Psychiatry, Icahn School of Medicine at Mount Sinai, New York, NY 10029; and <sup>g</sup>Departments of Psychology and Psychiatry, University of Wisconsin–Madison, Madison, WI 53706

Preprint server: This paper was submitted to bioRxiv on 5/10/2024 with distribution license: CC BY-NC-ND.

Author contributions: R.J.D. and F.P. designed research; J.Y., A.W., H.S.M., F.P., and I.S. provided/contributed funding; L.T., A.S., and L.N.M. collected the data; L.M., A.W., H.S.M., and I.S. guided data acquisition; C.M. analyzed the data, with assistance from J.Y. and supervision from I.S. and C.M., D.D.C., F.P., and I.S. interpreted the data and wrote the manuscript.

Competing interest statement: F.P. is a paid speaker for NeuroPace. Remaining authors declare no competing interests.

This article is a PNAS Direct Submission.

Copyright © 2025 the Author(s). Published by PNAS. This open access article is distributed under Creative Commons Attribution-NonCommercial-NoDerivatives License 4.0 (CC BY-NC-ND).

<sup>1</sup>To whom correspondence may be addressed. Email: ignacio.saez@mssm.edu.

This article contains supporting information online at <https://www.pnas.org/lookup/suppl/doi:10.1073/pnas.2409423122/-/DCSupplemental>.

Published February 4, 2025.

modulation in associated neural circuits has not been determined. In addition, the involvement of other frequency bands (e.g.,  $\beta = 12$  to 30 Hz) in limbic regions remains unclear, despite their role in emotional regulation and mood processes (20–22). Meditation has been associated with modulating local neuronal activity (2–4), measured by oscillatory power estimates (23), and decreased population synchrony within and between discrete regions (16, 17), measured by the duration of rhythmic, oscillatory episodes (24).

Therefore, despite its importance, the anatomically precise and physiologically detailed neural basis of meditative practice remains to be determined, especially in deep brain areas that are inaccessible to non-invasive electrophysiological recording methods. This, in turn, limits our understanding of the neural changes associated with the positive impacts of meditative practices and the development of generalizable insights that may be useful for therapeutic development. Neurosurgical interventions for the management of epilepsy allow recording from such areas in humans, including recording local field potentials (LFPs) capturing circuit activity directly via intracranial depth leads with great electrophysiological detail and signal to noise ratio (25), and providing a unique opportunity to study the neural basis of human behavior and thought. However, the most common settings for these invasive recordings, during drug-resistant epilepsy (DRE) patients' hospitalization (e.g., in the Epilepsy Monitoring Unit), are not ideal for the study of meditation because of their perioperative nature and the lack of an adequate environment for calm meditative practices. In contrast, responsive neurostimulation (RNS) system (NeuroPace Inc.) allows chronic electrophysiological brain recordings from implanted regions, frequently from the mesial temporal lobe structures of the hippocampus and amygdala (26), during the patients' daily life after surgery. This allows combining intracranial recordings with the practice of meditation in a controlled setting providing adequate environmental conditions for the practice of meditation.

Patients implanted with the RNS device can move around freely while continuous iEEG activity is recorded as LFPs. Recordings made with the RNS also offer high-quality data from deep brain structures, implicated in emotional regulation, such as the mesial temporal lobe (27). This is a major advantage in contrast to meditation studies using scalp surface EEG, which have significantly lower signal-to-noise ratio and do not allow the high simultaneous spatial and temporal resolution of RNS iEEG recordings (28). Patients implanted with the RNS are thus ideal candidates for investigating the neural correlates of naturalistic behavior, such as meditation (29, 30). In addition, DRE patients often suffer from psychiatric comorbidities including depression and anxiety (31), which provides an opportunity to study the relationship between intracranial activity and comorbid state, as well as the potential modulation during meditation.

We therefore explored changes in neural oscillatory activity associated with LKM within the amygdala and hippocampus using iEEG in DRE patients chronically implanted with an RNS device. Our findings show that first-time LKM modulates frequency-specific power and duration of oscillatory events in the hippocampus and amygdala. The selective nature of these findings in regard to the modulation of periodic, but not aperiodic, features of the neural signal reveals potential biomarkers by which LKM, a readily accessible therapeutic technique, noninvasively modulates physiological processes associated with mood regulation (20–22) even in first-time meditators.

## Results

Participants included eight neurosurgical patients with DRE who were chronically implanted with the NeuroPace Responsive Neurostimulation System (RNS). Participants completed the

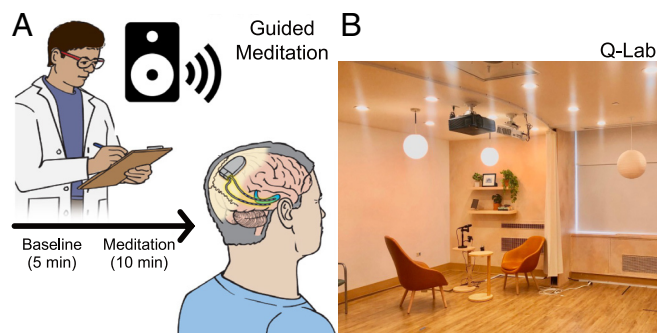
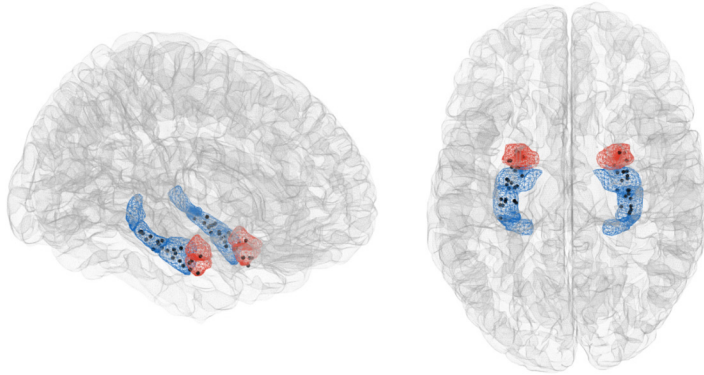


**Fig. 1.** Behavioral methods. (A) Experimental design. Subjects ( $n = 8$ ) completed a loving-kindness meditation (LKM) paradigm consisting of 5 min of audio-guided instruction (baseline) and 10 min of audio-guided LKM. (B) Experimental setting. The experimental paradigm was administered in Mount Sinai West's Q-Lab, a dedicated, immersive research environment designed to provide participants with a restorative space to participate in this experiment.

present study in Mount Sinai's Quantitative Biometric Laboratory (Q-Lab), designed to provide patients with a relaxing environment to receive therapeutic treatment free from typical distractors associated with a hospital setting and therefore highly conducive to engaging in meditative practice (Fig. 1B). Participants were self-reported novice meditators prior to the present study and completed a 5-min audio-guided instruction (baseline) followed by 10 min of audio-guided LKM (*Materials and Methods*). To evaluate the LKM induction, participants were asked to self-report their experienced depth of meditation following the session using a 1 to 10 scale (higher score = deeper meditation). On average, participants reported a high degree of meditation (mean = 7.43, SD = 2.50; *SI Appendix, Fig. S1*).

We analyzed LFPs by creating bipolar derivations between the two most anterior contacts (typically located in the amygdala and anterior hippocampus) and the two most posterior contacts (the middle-posterior hippocampus). Therefore, we collected two bipolar channels (one anterior pair and one posterior pair) per hemisphere implanted with RNS. Six patients had bilateral RNS implantations, and two patients had unilateral RNS implantation (left hemisphere). The electrode implant sites were determined solely based on clinical criteria, with the amygdala contacts being bipolar referenced to the anterior hippocampus. For readability, we refer to these bipolar recordings as “amygdala.” In contrast, the electrode pairs referred to as “hippocampus” represent hippocampus–hippocampus bipolar derivatives, enabling us to distinguish activity originating specifically from the hippocampus from signals that include unique contributions from the amygdala. All participants included in the present study had at least one contact in either the amygdala or hippocampus (count: amygdala = 14 electrodes/13 bipolar channels; hippocampus = 36 electrodes/14 bipolar channels; Fig. 2A). Because of hardware limitations on the sampling rate of the recorded electrophysiological data (125 Hz maximum), we restricted our analyses to frequencies up to low gamma (55 Hz). Anatomical localization of electrodes was determined by coregistering high-resolution postoperative CT scans with preoperative MRI (*Materials and Methods*). Although RNS implantation occurs in DRE patients' presumptive seizure onset zone, the leads which are composed of 4 contacts typically span just over 30 mm of tissue (1.5 mm in length for each contact and 10 mm between contact centroids). This results in a proportion of data recorded from likely normative tissue (29, 30). To mitigate the influence of interictal noise in the data, we implemented a data preprocessing approach mentioned in previous publications (32). Briefly, following visual inspection of all channel data, we confirmed the absence of any stimulation artifacts and eliminated

A



B

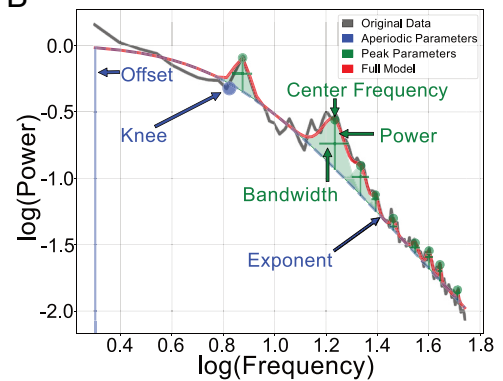


**Fig. 2.** Neural methods. (A) Anatomical reconstruction showing the hippocampal and amygdala location of RNS contacts. Depicted is the placement of 50 NeuroPace RNS electrodes in the amygdala (blue) and hippocampus (red) across eight participants. Each black dot corresponds to one electrode (amygdala = 14 electrodes/13 bipolar channels; hippocampus = 36 electrodes/14 bipolar channels). (B) FOOOF approach. We characterized LFP activity from bipolar channels recorded from depth electrodes in the amygdala and hippocampus. We used the FOOOF approach to separately characterize aperiodic (i.e.,  $1/f$  background activity) from oscillatory neural activity. Depicted is an example power spectrum from one hippocampal channel (gray trace) overlaid by the FOOOF fitted model (red trace) parameterized to extract aperiodic (blue trace) and periodic (green trace) spectral features between 2 and 55 Hz. The aperiodic components are characterized by the offset, knee, and exponent. Periodic components are assigned to a canonical frequency band ( $\delta = 2\text{--}4\text{ Hz}$ ,  $\theta = 4\text{--}8\text{ Hz}$ ,  $\alpha = 8\text{--}13\text{ Hz}$ ,  $\beta = 13\text{--}30\text{ Hz}$ ,  $\gamma = 30\text{--}55\text{ Hz}$ ) depending on their center frequency, and their power and bandwidth estimated.

any data meeting clinical criterion for interictal discharge (33). This resulted in discarding approximately 6% of the data. The proportion of time across participants in which interictal activity was detected was not significantly different between conditions (baseline and meditation;  $P > 0.05$ , Pearson's chi-square goodness-of-fit test; *SI Appendix, Fig. S2A*). The proportion of omitted data from the entire experimental session ranged from 2 to 16% across participants (*SI Appendix, Fig. S2B*).

**LKM Was Not Accompanied by Changes in Aperiodic Neural Activity.** We set out to identify whether meditation was accompanied by changes in neural activity by comparing LFP activity patterns between active control (learning about meditation) and LKM epochs. Given the largely temporally unresolved nature of these data, we chose to focus our analysis on the power profile throughout a single epoch during the meditation block, examining both aperiodic ( $1/f$  profile) and periodic (i.e., oscillatory) neural activity on each bipolar channel. We parameterized the aperiodic and periodic features of the power spectra using the 'fitting oscillations and one over  $f$ ' method (FOOOF; see *Materials and Methods* and Fig. 2B) (23). The FOOOF model fit was performed for each channel's data in each condition (baseline and meditation). The aperiodic components include a knee parameter, which accounts for an often-observed bend in the  $1/f$  profile, and offset and exponent, which reflect the y-intersect and rate of decay of the  $1/f$  profile, respectively. Together, these aperiodic components capture broadband shifts in the  $1/f$  profile often ascribed to changes in excitatory/inhibitory balance, different and separate from oscillations in individual frequency bands. In addition, oscillatory components were estimated for predefined frequency bands ( $\delta = 2\text{--}4\text{ Hz}$ ,  $\theta = 4\text{--}8\text{ Hz}$ ,  $\alpha = 8\text{--}13\text{ Hz}$ ,  $\beta = 13\text{--}30\text{ Hz}$ ,  $\gamma = 30\text{--}55\text{ Hz}$ ; see *Materials and Methods*).

We first sought out to identify whether acute LKM induced changes in the aperiodic features of the power spectra by comparing knee frequency, offset, and exponent separately between baseline and LKM epochs (Fig. 4). We did not find significant differences between conditions in knee frequency, offset, or exponent in either the amygdala or hippocampus (all  $P > 0.05$ , two-sided paired-samples Wilcoxon signed rank test; Fig. 3), suggesting that meditation is not accompanied by general changes in the excitatory/inhibitory profile of either amygdala or hippocampus. Further, we found no significant differences in aperiodic

components between the amygdala and hippocampus (all  $P > 0.05$ , two-sided Wilcoxon signed rank test; *SI Appendix, Fig. S3*).

**LKM Was Not Accompanied by Changes in the Proportion of Electrodes Showing Oscillatory Activity.** Next, we evaluated whether LKM was accompanied by changes in oscillatory neural activity by examining power across frequencies in baseline and meditation conditions. We considered a significant oscillation to be present if at least one peak within predefined frequency bins ( $\delta = 2\text{--}4\text{ Hz}$ ,  $\theta = 4\text{--}8\text{ Hz}$ ,  $\alpha = 8\text{--}13\text{ Hz}$ ,  $\beta = 13\text{--}30\text{ Hz}$ ,  $\gamma = 30\text{--}55\text{ Hz}$ ) was detected by the FOOOF model fit. If no peak was found within a given frequency range for a channel, we considered the channel to not contain an oscillation in that band. Therefore, we started by quantifying the proportion of channels containing active oscillations across conditions. We observed differences in the proportion of active channels across frequencies between conditions in both amygdala and hippocampus, with higher frequencies containing a larger proportion of active channels than lower frequencies (Fig. 4). The lowest proportion of active electrodes was in  $\delta$  in both amygdala (30.8%) and hippocampus (35.7%); the highest was in  $\beta$  and  $\gamma$  in both regions (100%). However, we did not find significant differences in the proportion of active electrodes between conditions in any frequency bands (all  $P > 0.05$ , Fisher's exact test). Therefore, LKM was not associated with an increase in the proportion of channels showing significant oscillations. These data indicate that our ability to detect significant oscillations was strongly frequency dependent, and that there was significant  $\beta$  and  $\gamma$  oscillatory activity in both baseline and in meditation conditions in the amygdala and hippocampus.

**LKM Was Associated with an Increase in  $\gamma$  Power.** To further investigate whether LKM modulated oscillatory activity, we compared the amplitude, or power, of detected oscillations between conditions in both regions (Fig. 5). To investigate between-condition differences in oscillatory power, we only considered channels in which at least one peak was detected in each frequency band (i.e., containing significant oscillatory activity). If more than one peak was found within a given frequency range, the average power of all detected peaks within the frequency band was computed to determine an average power score. We observed a significant increase in  $\gamma$  power during LKM in both the amygdala ( $P < 0.01$ , one-sided paired-samples Wilcoxon

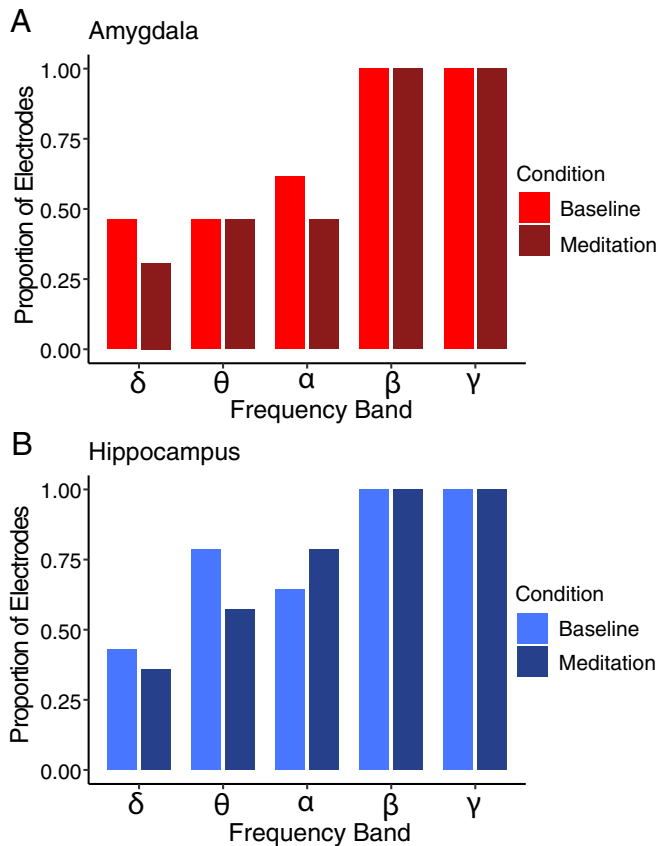


**Fig. 3.** No difference in aperiodic neural components between baseline and meditation epochs. The aperiodic components of FOOOF model fit (knee frequency, offset, and exponent) was extracted and compared between conditions (FA meditation and baseline). (A) No differences in FOOOF aperiodic parameters in amygdala channels. No significant differences in knee frequency, offset, or exponent of FOOOF model fit for amygdala channels ( $n = 13$  bipolar channels) were observed between conditions (all  $P > 0.05$ , Fisher's exact test). (B) No differences in FOOOF aperiodic parameters in hippocampus channels. No significant differences in knee frequency, offset, or exponent of FOOOF model fit for hippocampus channels ( $n = 14$  bipolar channels) were observed between conditions (all  $P > 0.05$ , Two-sided paired sample Wilcoxon signed-rank test).

signed rank test, Fig. 5A) and hippocampus ( $P < 0.001$ , one-sided paired-samples Wilcoxon signed rank test, Fig. 5B). We did not observe concomitant changes in  $\beta$  ( $P > 0.05$ , one-sided paired-samples Wilcoxon signed rank test, Fig. 5) or any other frequency bands (all  $P > 0.05$ , two-sided paired-samples Wilcoxon signed rank test, Fig. 5), indicating that this modulation was specific to the  $\gamma$  frequency band. Overall, these results reveal that LKM is accompanied by changes in oscillatory power in active channels, but not an increase in the proportion of active channels. Furthermore, these changes are specific to high-frequency activity ( $\gamma$ ) and not present in lower frequencies. We did not find differences in baseline oscillatory power or the difference in oscillatory power from baseline to meditation between the amygdala and hippocampus (all  $P > 0.05$ , two-sided Wilcoxon signed rank test; *SI Appendix, Figs. S4A and S5A*).

To examine the significance of power modulations at the subject level, we performed subject-level analyses of power differences by leveraging the high temporal resolution of the iEEG data. We focused our model-free analysis on the beta and gamma frequency bands, as our FOOOF model fitting confirmed the presence of both beta and gamma oscillations across all channels in both baseline and LKM conditions. Briefly, we estimated power for 1-s neural recording segments across all channels for each subject.

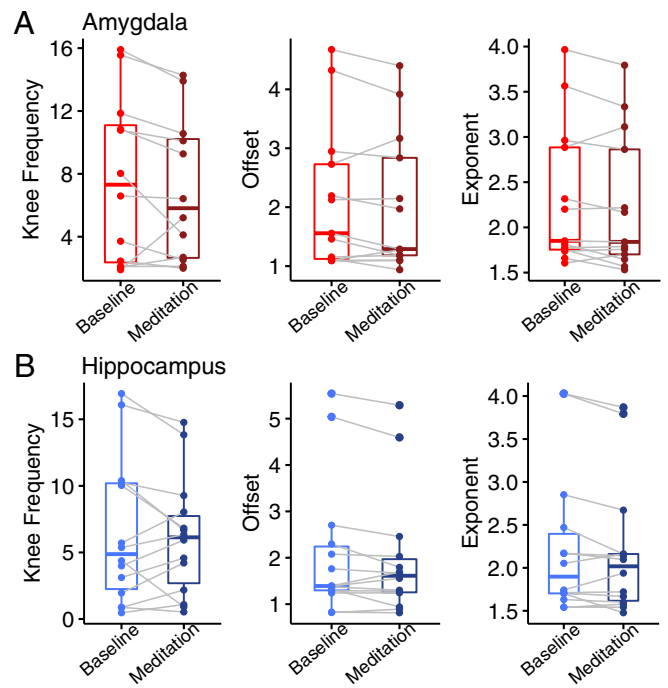


**Fig. 4.** Proportion of channels showing neural oscillations varied across frequency bands. Plotted is the proportion of channels in which an oscillation was detected during baseline and meditation epochs in each frequency band ( $\delta = 2-4$  Hz,  $\theta = 4-8$  Hz,  $\alpha = 8-13$  Hz,  $\beta = 13-30$  Hz,  $\gamma = 30-55$  Hz) according to FOOOF power spectrum model fit. (A) Proportion of amygdala channels showing significant oscillatory activity across frequencies. The proportion of channels showing significant modulation varied between ~30% in  $\delta$  (2 to 4 Hz) and 100% in  $\gamma$  (30 to 55 Hz), with greater proportions for higher frequencies. There were no differences in the proportion of amygdala channels ( $n = 13$  bipolar channels) in which oscillations were detected between baseline (light blue) and meditation (dark blue) epochs (all  $P > 0.05$ , Fisher's exact test). (B) Proportion of hippocampal channels showing significant oscillatory activity across frequencies. The pattern of activation was like that observed in the amygdala, with the proportion of channels ranging between ~30% in  $\delta$  (2 to 4 Hz) and 100% in  $\gamma$  (30 to 55 Hz), with greater proportions for higher frequencies. There were no differences in the proportion of hippocampal channels ( $n = 14$  bipolar channels) in which oscillations were detected between baseline (light blue) and meditation (dark blue) epochs (all  $P > 0.05$ , Fisher's exact test).

LKM segments were z-scored relative to baseline segments, providing a normalized measure of LKM-induced changes in each frequency band. As anticipated, we observed a significant increase in gamma power during LKM in both the amygdala (Fig. 6A) and hippocampus (Fig. 6A) for most subjects (amygdala: 6/8 participants; 75%; hippocampus: 6/7 participants; 86%). In contrast, there was no significant difference in beta power during LKM compared to baseline in either region for most subjects (both  $P > 0.05$ , Fig. 6B). These results align with the group-level, model-based findings, further supporting a significant LKM-associated increase in gamma power, and provide limited evidence for modulations in beta power in some, but not all, patients.

**LKM Was Accompanied by an Alteration in Duration of  $\beta$  and  $\gamma$  Bursts.** The FOOOF method allowed us to investigate aperiodic and periodic components of brain activity but does not offer a way to quantify quick bursts of neural activity which may be important to facilitate switches in cognitive states (e.g., from baseline to LKM). To investigate this possibility, we applied the extended Better Oscillation detection (eBOSC) method (24, 34), to investigate how meditation modulated the duration of oscillations across frequency bands (*Materials and Methods*). eBOSC allows us to detect temporal windows with significant frequency-specific

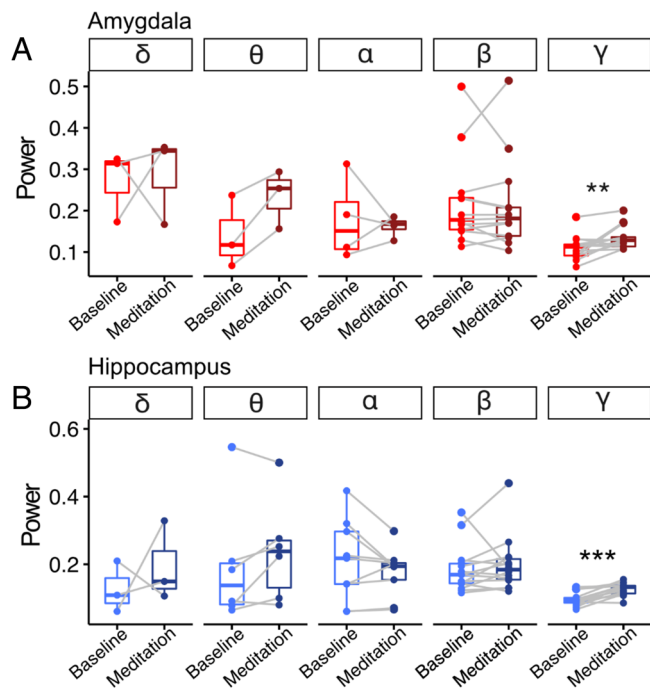


**Fig. 5.** Group-level increased  $\gamma$  oscillatory power in meditation compared to baseline. We examined power modulation across conditions (baseline versus LKM) by averaging spectral power estimates (the periodic component of FOOOF model fit) within frequency bands ( $\delta = 2-4$ ,  $\theta = 4-8$ ,  $\alpha = 8-13$ ,  $\beta = 13-30$ ,  $\gamma = 30-55$ ) and compared across conditions. For this analysis, we employed only the subset of channels that showed significant oscillations in both conditions, which varied across frequency bands. (A) Increased  $\gamma$  oscillatory power in amygdala electrodes during meditation. We observed a significant increase in amygdala  $\gamma$  power (30 to 55 Hz) during LKM compared to baseline ( $P < 0.01$ , one-sided paired-samples Wilcoxon signed rank test; all other frequency bands  $P > 0.05$ ). (B) Increased  $\gamma$  oscillatory power in hippocampal channels during meditation. As in the amygdala channels, we observed a significant increase in hippocampus  $\gamma$  power (30 to 55 Hz) during LKM compared to baseline ( $P < 0.001$ , one-sided paired-samples Wilcoxon signed rank test; all other frequency bands  $P > 0.05$ ).

oscillations that surpass power and duration thresholds while accounting for the background  $1/f$  profile of the neural signal (24). Further, recent work has implemented this method with hippocampal iEEG data collected using the RNS device, allowing us to compare our findings with previously published iEEG work (30). Using eBOSC, we calculated the proportion of time within a given experimental condition (baseline or LKM) in which a particular oscillation was detected. We averaged these proportions for each frequency in each of our predefined frequency bands and compared between conditions to identify whether LKM induced changes in the duration of oscillatory events (Fig. 7). We found that LKM was associated with a significant decrease in the duration of  $\beta$  oscillations in both the amygdala ( $P < 0.05$ , one-sided paired-samples Wilcoxon signed rank test, Fig. 7A) and hippocampus ( $P < 0.05$ , one-sided paired-samples Wilcoxon signed rank test, Fig. 7B). Further, we found a significant increase in the duration of  $\gamma$  oscillations during LKM in the amygdala ( $P < 0.01$ , one-sided paired-samples Wilcoxon signed rank test, Fig. 7A). Additionally, the amygdala displayed a significantly greater increase in the duration of  $\gamma$  oscillations during meditation compared to the hippocampus ( $P < 0.05$ , one-sided Wilcoxon signed rank test, *SI Appendix, Fig. S5B*; all other frequency bands  $P > 0.05$ ). Overall, these results demonstrate a decrease in the amount of  $\beta$  events during meditation in both amygdala and hippocampus, and an increase in  $\gamma$  events in the amygdala, suggesting an involvement of fast oscillatory events in meditative states. We did not find differences in baseline oscillatory duration

between the amygdala and hippocampus (all  $P > 0.05$ , two-sided Wilcoxon signed rank test; *SI Appendix, Figs. S4B and S5B*).

## Discussion

This study leveraged unique access to chronic ambulatory iEEG recordings in the amygdala and hippocampus during LKM. We directly examined the nature of neurophysiological activity during LKM in the amygdala and hippocampus, finding primary results of increased  $\gamma$  oscillations and decreased  $\beta$  duration during LKM. Further, changes in neural dynamics with meditation occurred in oscillatory activity, rather than in aperiodic neural activity. Research on the effects of meditation on neural dynamics to date has been limited to fMRI and scalp EEG, due to rare access to iEEG in real-world settings. While such approaches have advanced the field of meditation, iEEG research can augment such data with increased spatial and temporal resolution.

Meditative practices have existed for millennia in different traditions (35) and allow humans to cultivate fundamental states of focus and emotional regulation (36). Meditation, perhaps independent of practice type, induces scalp EEG increases in  $\gamma$  activity (11). In addition, meditation induces changes in BOLD-fMRI signal in the hippocampus and amygdala (13, 37), which could correlate with changes in  $\gamma$  oscillatory activity (15). Our study directly addresses the nature of intracranial electrophysiology within the hippocampus and amygdala during meditation. Our focus on LKM comes from previous research that connects this emotionally laden contemplative practice to the amygdala (13). LKM, utilized in this study, stresses finding joy and sharing it with others (10). Such constructive contemplative practices have been shown to induce positive emotions, which may lead to an increased sense of purpose and meaning in life (38). Such training has also been shown to chronically modulate the amygdala, hence of specific interest in our cohort where contacts were situated in the basolateral amygdala in all cases (13). Yet, no experiments to date have attempted to record such changes in novice meditators acutely and intracranially. These findings complement the earlier results on increased  $\gamma$  oscillations in LKM practices in long-term meditators by showing specific increases in these fast oscillations in novice meditators when directly examining the amygdala and hippocampus with iEEG.

**Amygdala and Hippocampus  $\gamma$  Power Increases During LKM.** By leveraging the spatiotemporal resolution afforded by iEEG, our results build on prior research on  $\gamma$  power increases associated with long-term LKM practice (3, 11, 39, 40) extending these findings to first-time meditators and providing insights into the nature of neural changes associated with meditation in an anatomically precise way. We observed an increase in amygdala and hippocampus  $\gamma$  power (Fig. 5), whose correlation to fMRI-BOLD signal is well established (15), suggesting LKM induces heightened activation of local neuronal ensembles within the amygdala and hippocampus. This meditation-induced neural modulation may be related to the known role in processing of emotional information in the amygdala and hippocampus (41), and possibly with related mental processes such as memory and attention. During LKM, participants are encouraged to actively retrieve positive autobiographical memories during LKM which induces amygdala and hippocampus activation (42). The hippocampus plays a critical role emotional regulation and attention (43, 44) alongside its fundamental roles memory consolidation and retrieval (45, 46), suggesting hippocampal activation may be related to the memory aspects of the meditative task. The amygdala, in turn, can direct attention toward emotionally significant stimuli (13, 45, 47), serving a critical function in the

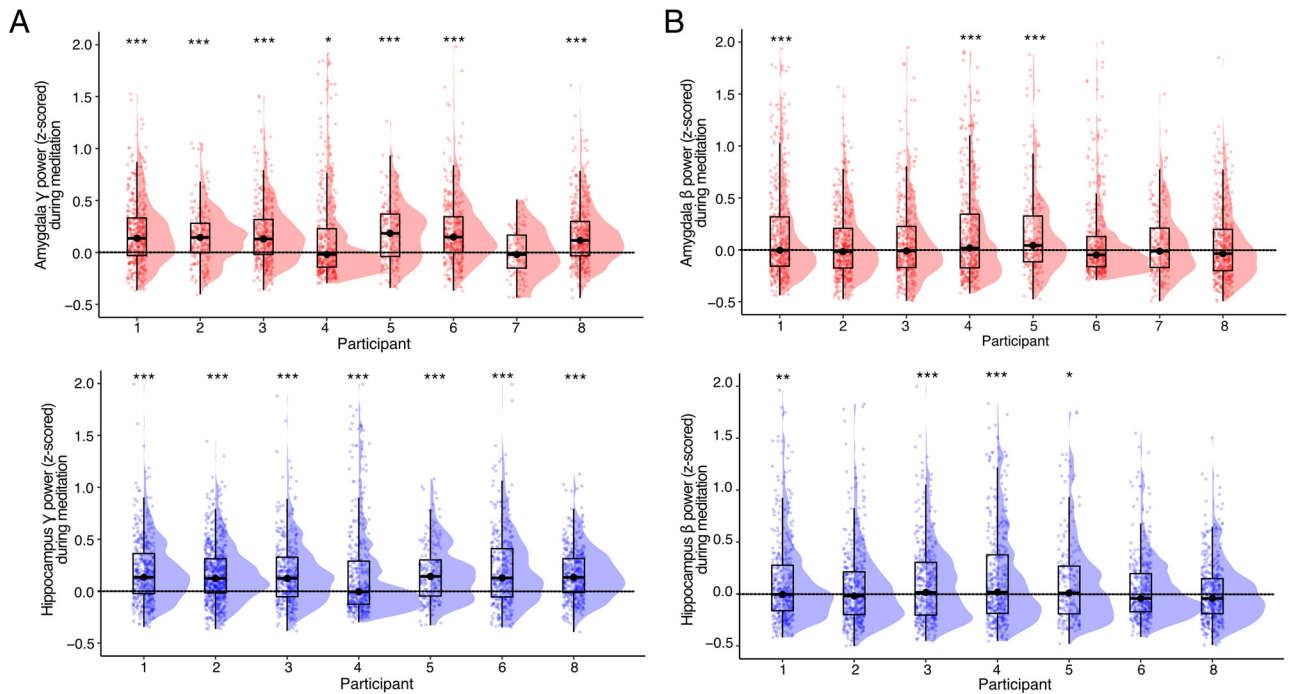


**Fig. 6.** Subject-level increased  $\gamma$  oscillatory power in meditation compared to baseline. We analyzed power modulation within subjects by dividing the LKM session into 1-s epochs and performing frequency decomposition to estimate  $\gamma$  and  $\beta$  power for each epoch. These epochs were then z-scored against the mean and SD of  $\gamma$  and  $\beta$  power during the baseline period (each point represents one 1 s epoch). A positive z-score indicates an increase in power during the LKM session relative to baseline. (A) Generalized gamma-band power increase in the amygdala and hippocampus. Most participants ( $n = 6/8$ , 75%) exhibited significantly greater amygdala  $\gamma$  power during meditation compared to baseline [one-sided one-sample Wilcoxon signed rank test; participant (median,  $P$ -value) = 1 (0.14,  $P < 0.001$ ), 2 (0.14,  $P < 0.001$ ), 3 (0.13,  $P < 0.001$ ), 4 (-0.02,  $P < 0.001$ ), 5 (0.18,  $P < 0.001$ ), 6 (0.15,  $P < 0.001$ ), 7 (-0.02,  $P > 0.05$ ), 8 (0.12,  $P < 0.001$ )]. Most participants ( $n = 6/7$ , 86%) exhibited significantly greater hippocampus  $\gamma$  power during meditation compared to baseline [one-sided one-sample Wilcoxon signed rank test; participant (median,  $P$ -value) = 1 (0.13,  $P > 0.05$ ), 2 (0.12,  $P > 0.05$ ), 3 (0.12,  $P > 0.05$ ), 4 (-0.01,  $P > 0.05$ ), 5 (0.14,  $P > 0.05$ ), 6 (0.13,  $P > 0.05$ ), 8 (0.13,  $P > 0.05$ )]. (B) Beta-band power modulation in the amygdala and hippocampus in a subset of patients. Only a minority of participants exhibit significantly different  $\beta$  power during meditation compared to baseline in the amygdala [3/8 patients; two-sided one-sample Wilcoxon signed rank test; participant (median,  $P$ -value) = 1 (-0.01,  $P < 0.001$ ), 2 (-0.02,  $P > 0.05$ ), 3 (-0.01,  $P > 0.05$ ), 4 (0.02,  $P < 0.001$ ), 5 (0.04,  $P < 0.001$ ), 6 (-0.05,  $P > 0.05$ ), 7 (-0.01,  $P > 0.05$ ), 8 (-0.04,  $P > 0.05$ )] or hippocampus [two-sided one-sample Wilcoxon signed rank test; participant (median,  $P$ -value) = 1 (-0.01,  $P < 0.01$ ), 2 (-0.02,  $P > 0.05$ ), 3 (0.01,  $P < 0.001$ ), 4 (0.02,  $P < 0.001$ ), 5 (0.01,  $P < 0.05$ ), 6 (-0.04,  $P > 0.05$ ), 8 (-0.04,  $P > 0.05$ )].

bottom-up processing of emotionally relevant information (48–50). We further identified an increase in the duration of  $\gamma$  oscillatory events during LKM compared to baseline in the amygdala, but not hippocampus (Fig. 7). This may reflect the specific physiological demands of LKM, wherein the hippocampus exhibits more transient  $\gamma$  bursts associated with memory retrieval (51) while the amygdala exhibits more sustained, rhythmic  $\gamma$  activity to support emotional processing (52).

**Amygdala and Hippocampus  $\beta$  Oscillatory Duration Decreases During LKM.**  $\beta$  oscillations reflect rhythmic phase-locked activity and are thought to facilitate long-range information exchange via cross-regional synchrony. The synchrony afforded by ongoing  $\beta$  oscillations poises neural ensembles to quickly reorganize and integrate incoming information. In human and nonhuman primates, synchrony in lower-frequency (i.e.,  $\beta$ ) oscillations is thought to modulate attention switches (18, 53). This physiological mechanism provides an attentional spotlight that facilitates effective information-gathering from the environment (19). This affordance is advantageous in circumstances which require real-time monitoring and adapting to one's environment. In contrast, one seeks to reduce the influence of external distractions during LKM. Therefore, our present findings of decreased  $\beta$  oscillatory duration during LKM compared to baseline support the notion that  $\beta$  oscillations are a physiological mechanism for long-range temporal synchrony that regulates selective attention in service of LKM. Transient  $\beta$  bursts, instead of sustained rhythmic oscillations, facilitate cognitive processes through functional

inhibition (51).  $\beta$  bursts dictate the spatial and temporal basis of activation relevant for memory- and attention-related processing, while gamma power reflects the processing itself (54). Increased cortical  $\beta$  oscillations have been correlated with negative mood disorders (22, 53, 55). Decreased  $\beta$  oscillations with LKM may also represent a shift from negative emotional states, in turn for more positively salient  $\gamma$  oscillations at the network level. Additionally, given the role of  $\beta$  oscillations in premotor preparation and the fact that LKM can be conceptualized as being action-oriented (56–59), it is possible that our observed  $\beta$  modulation reflects a motor plan in its preparatory stages. These group-level changes in beta oscillatory duration were associated in some patients with modulations in beta power (Fig. 6), suggesting that interpatient heterogeneity may play a role in shaping these neural responses.

**Meditation Does Not Affect Aperiodic Activity or Differentially Impact the Hippocampus versus Amygdala.** Our finding that meditation was not accompanied by changes in aperiodic neural activity suggests that any LKM practice-induced neural fluctuations are specifically related to oscillatory events, not other physiological processes (Fig. 3). We did not find differences in any oscillatory metric (periodic/aperiodic FOOOF metrics or eBOSC) between the amygdala and hippocampus. This may indicate they are similarly modulated, with an important caveat that our amygdala contacts are bipolar referenced to the head of the hippocampus. Such confounds may be overcome in future experiments with adjustments of the recording paradigms of the RNS to monopolar, yet, at this time are beyond the scope of this paper.

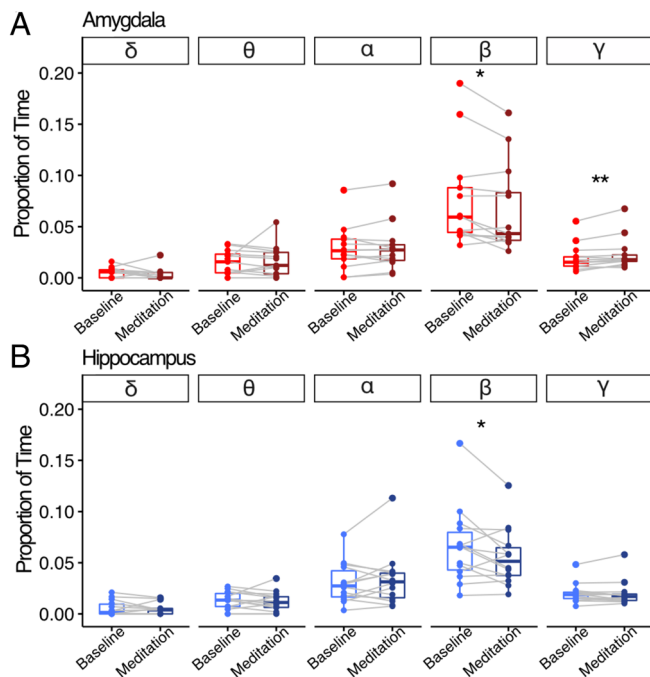


**Fig. 7.** Modulation of oscillatory duration across meditation states. We used a rhythm detection method (eBOSC) to determine the duration of rhythmic, oscillatory activity. Estimates of oscillatory duration were averaged within frequency bins ( $\delta = 2-4$ ,  $\theta = 4-8$ ,  $\alpha = 8-13$ ,  $\beta = 13-30$ ,  $\gamma = 30-55$ ) and compared between conditions. (A) Amygdala channels showed a decrease in  $\beta$  and an increase in  $\gamma$  oscillation duration. The duration of amygdala  $\beta$ -range oscillatory activity during LKM decreased compared to baseline ( $P < 0.05$ , one-sided paired-samples Wilcoxon signed rank test), and the duration of amygdala  $\gamma$ -range oscillatory activity during LKM increased compared to baseline ( $P < 0.01$ , one-sided paired-samples Wilcoxon signed rank test; all other frequency bands  $P > 0.05$ ). (B) Hippocampus channels showed a decrease in  $\beta$  oscillation duration. The duration of hippocampal  $\beta$ -range oscillatory activity during LKM decreased compared to baseline ( $P < 0.05$ , one-sided paired-samples Wilcoxon signed rank test; all other frequency bands  $P > 0.05$ ).

**Naturalistic Study on the Neural Correlates of Meditation.** This work on the neural correlates of meditation using RNS has a multitude of advantages over other approaches. Mainly, the RNS allows detailed spatiotemporal study of deep brain structures in a naturalistic setting. While work from fMRI and other neuroimaging studies have gleaned important findings, they are limited in their temporal resolution. Clinically relevant findings from these studies, such as biofeedback for treatment of negative emotions (45), are difficult outside of the naturalistic setting, as with RNS. Our work builds on the uses of RNS to study the neural basis of human brain function in the naturalistic setting, which has been implemented for tasks ranging from spatial navigation (30, 60), to speech (61).

**Study Limitations.** Our experimental design results in several limitations of this study. First, the technical limitations of the RNS device (which is limited to a 250 Hz sampling rate) imposed an upper limit on the frequency bands that could be resolved, and therefore we could not fully estimate the effects of meditation on broadband high-frequency activity (typically 70 to 200 Hz), a marker of local activation (32, 62). We were, however, able to estimate gamma activity (30 to 55 Hz), which also acts as a proxy for local cortical activation (63, 64). Second, because of the limited time available for patient testing, the experimental paradigm did not include a post-meditation active control period, limiting our ability to test for postmeditation baseline changes as reported in previous studies (3). Similarly, the one-shot design limits our ability to draw conclusions regarding

the chronic effects of meditation practice. Our ability to draw conclusions regarding the generalizability of findings is limited by experimental constraints with a clinical sample as baseline period could only consist of a single session at the start of the meditation phase, during which participants listened to audio instructions about meditation, and we did not include multiple baseline periods for further comparison. Whereas it is possible that the observed neuromodulation reflects the influence of factors beyond LKM, the main difference between the active control baseline and the LKM period was the meditation practice itself. Participants maintained the same seated position, received the same quality of audio prompts, and were exposed to the same environmental stimuli in both conditions. Future studies could benefit from incorporating multiple control sessions, a more robust baseline period, counterbalanced order of baseline and meditation periods, and additional forms of meditation or relaxation practice to better isolate the specific contributions of LKM to the observed effects. Third, by including the knee parameter in our FOOOF model fit, we avoid assuming the aperiodic component of the power spectra maintain a single  $1/f$ -like characteristic, as this assumption is often violated across broad frequency ranges ( $\sim$ greater than 40 Hz). While providing a better fit to the data, this model fitting choice may exhibit a bias against lower frequencies, potentially explaining the disproportionate detection of peaks at higher frequencies compared to lower ones in the present analysis. Additionally, the lack of a relationship between self-reported depth of meditation and neurophysiological metrics raises the question of whether participants genuinely engaged in meditation, and the challenges of estimating internal states in a non-intrusive way. More generally, it is possible that our observed neural changes reflected generalized changes in states of arousal or affect. The addition of neurophysiological measures such as heart rate or skin conductance, would help relate amygdala and hippocampal activation to less invasive physiological metrics and help determine the specificity of neural activation versus more general metrics, e.g., arousal. Finally, because of the difficulties of recruiting RNS patients, our study was necessarily limited to a small patient sample ( $n = 8$ ). This is a common limitation of intracranial studies in general, and RNS studies in particular, which often have similar or, frequently, smaller number of patients compared to our study (29, 65). In addition, this concern is alleviated by the significant homogeneity in electrode placement, which limits cross-patient anatomical variability compared to other invasive studies (e.g., sEEG) and by the great signal-to-noise ratio of intracranial recordings, which allowed us to carry out group-level inferences (e.g., Fig. 5).

**Study Strengths.** This study has several key strengths. First, the use of intracranial recordings offers high spatial and temporal precision, allowing for direct measurement of brain activity in subcortical regions, such as the amygdala and hippocampus, which are known for their roles in emotion regulation and memory. These processes are thought to be triggered by LKM practice but specific neuronal activation of these regions during LKM are difficult to measure with non-invasive methods. Additionally, the RNS system enables data collection from fully ambulatory participants, allowing the study to take place in a naturalistic setting. This improves the study's ecological validity by recording direct brain activity while participants behave in conditions that closely resemble a real-world meditation setting. Finally, the statistical methods used in this study account for both periodic and aperiodic neural activity, offering a detailed and mechanistic understanding of how LKM affects the brain.

**Future Directions.** These results are the first to document acute intracranial electrophysiology changes with LKM. Specifically, we see an increase in  $\gamma$  oscillations and a decrease in  $\beta$  burst duration in the amygdala and hippocampus with LKM. While we observe acute changes in amygdala and hippocampal electrophysiology during LKM, we did not assess long-term changes that may occur with LKM practice. The meditation literature has defined “state changes” as temporary modulations of mind (and implicitly brain function) that occur with meditation, versus trait changes as long-term, enduring effects of meditation on the mind (and thus brain) (65). Our research documents brain signals that may contribute to the acute state changes of LKM but does not explore long-term brain changes that may underlie traits unique to long-term meditators. Yet, the RNS system enables long-term tracking of electrophysiology, which may be applied over the course of a novice meditator’s practice as they journey to a higher level of expertise. Further, alternative forms of meditation, such as mindfulness, may be similarly assessed to determine the varying effects of meditation practice on brain state and trait changes. The work presented here focuses on hippocampal and amygdala electrophysiology, as these are the typical targets of RNS implantation for epilepsy. Complementary studies on intracranial EEG recordings in patients implanted with a wider range of contact locations for seizure localization (sEEG) may provide additional insight into the circuit-level activity changes associated with meditation. We feel both approaches are complementary and will improve future investigations via a feedback loop. There thus remains an exciting opportunity for exploration on how meditation practice exerts acute state changes and long-term trait changes through modulation of intracranial electrophysiology in the human brain.

**Summary.** Our findings reveal increased hippocampal and amygdala  $\gamma$  power associated with LKM, and amygdala-specific increases in  $\gamma$  oscillation duration. Further, we identified a global decrease in amygdala and hippocampus  $\beta$  oscillatory duration during LKM. These findings provide anatomically localized and neurophysiologically detailed for the role of these regions in meditation and suggest an association with their known roles in memory and emotional regulation processes. In addition, they confirm the potential of first-time LKM practice to induce transient physiological alterations in brain regions whose maladaptive functioning is implicated in mental health disorders. By identifying physiological mechanisms that are amenable to noninvasive neuromodulation via LKM, we highlight LKM’s potential as a targeted therapeutic intervention.

## Materials and Methods

**RNS Participants.** Eight DRE patients participated in the present study ( $n = 3$  female, mean age =  $44.75 \pm 7.67$  y). All participants had been previously implanted with the NeuroPace RNS System to treat DRE. Electrode placement was solely determined by clinical criterion. A structured clinical interview was conducted based on the NIH Common Data Elements Battery for Epilepsy Patients prior to participation. Participants provided informed consent for participating in the present study which was approved by the Mount Sinai Institutional Review Board.

**RNS Data Acquisition.** RNS is an FDA-approved chronically implanted invasive intervention to treat patients with DRE by continuously monitoring for abnormal electrical activity and delivering electrical stimulation to circumvent seizure onset (Fig. 1A). RNS devices provide access to intracranial LFP activity from the stimulating electrode in postsurgical, chronic conditions, which provides an opportunity to record intracranial LFP data from deep brain regions. iEEG storage in the RNS Neurostimulator was manually triggered by the experimenter to mark the start and end of the experimental session. During the experimental session, the RNS Neurostimulator continuously recorded iEEG activity in two (unilateral

implantation) or four (bilateral implantation) bipolar channels depending on each patient’s electrode placement. Bipolar derivations were carried out between the two most anterior and the two most posterior channels, typically implanted along the anterior–posterior axis of the amygdala–hippocampus (Fig. 2A). iEEG activity was continuously recorded from all available bipolar channels across two depth electrode leads in each patient at a sampling frequency of 250 Hz.

**Behavioral Task.** The experimental session consisted of a 15-min audio-guided meditation paradigm. All experimental sessions occurred in Mount Sinai’s Quantitative Biometrics Laboratory (Q-Lab) which was designed to emulate Japanese teahouses and gardens, affording patients a restorative environment for participation (Fig. 1B). The present study’s LKM paradigm was an audio-only prerecording to ensure standardization across participants. The recording utilized material from the Healthy Minds Program and Mindfulness-Based Stress Reduction course through Palouse Mindfulness. Both programs provide open-source, empirically evidenced LKM resources (10). The recording was performed by a neuropsychologist with specialist training Acceptance and Commitment Therapy, a psychological intervention that utilizes mindfulness, and experience in facilitating meditation sessions for epilepsy patients. An experimenter was present for each experimental session to monitor potential seizure activity. The meditation paradigm began with 5 min of audio-guided instruction during which participants passively listened to discussion of meditation’s objective and were guided in best practices for engaging effectively in LKM. This period was considered baseline in further analysis. Instruction was followed by 10 min of LKM during which participants were guided to wish well to oneself and then others by first imagining that “you are filled and overflowing with warmth and love” and then repeating phrases silently, such as “may you live with ease, may you be happy, may you be free from pain.” The meditation builds from receiving loving kindness directed at oneself followed by sending loving kindness to loved ones, neutral people, and all living beings (see *SI Appendix* for complete transcript). Through active attention regulation, practitioners to exert top-down attention on a target object while disengaging attentional resources from irrelevant objects (66). The goal-directed modulation of attention and its neural underpinnings has been well characterized in humans (67). Until now, significant technical limitations have prevented the direct recording of neural activity with the spatial and temporal resolution necessary to potentially detect neurophysiological fluctuations induced by meditative states, especially in novice meditators. RNS patients present a unique opportunity to record intracranial electrophysiology (iEEG) in freely behaving, postoperative humans. For these reasons, we chose to focus the present iEEG study on LKM. Participants remained seated for the duration of the experimental session. For analysis purposes, the first 2 min of instruction were selected as the baseline epoch, and 2 min in the middle of meditation during each patient’s experimental session were selected as the meditation epoch for comparison. These conditions were referred to as baseline and meditation, respectively.

**Analysis.** Analyses were performed with custom MATLAB (electrode localization), Python (iEEG preprocessing/quantification, visualization, and statistics), and R (statistics and visualization).

**Electrode Localization and iEEG Preprocessing.** Electrode localization was performed with MATLAB LeGUI. We coregistered each participant’s postoperative CT image to their preoperative whole brain MRI. All electrodes determined to be in the amygdala or hippocampus following localization were included in further analysis (amygdala: electrode, bipolar channels; hippocampus: electrodes, bipolar channels). The anatomical location of each electrode was determined using the Yale Brain Atlas (68), a whole-brain atlas of the human cortex, hippocampus, amygdala created using 3,866 electrodes across 25 iEEG subjects, and verified through visual examination. Epileptic or noisy activity was manually removed following visual inspection of each channel similar to previously published methods (32). Similar to previous results (29, 30, 32), we excluded ~6% of the data from further analyses due to the presence of epileptic or noisy activity. The proportion of excluded data across amygdala and hippocampus channels was not significantly different between conditions ( $P > 0.05$  for all channels, Pearson’s chi-square goodness-of-fit test).

**Quantifying Oscillatory Prevalence, Power, and Duration.** We computed the power spectral density (PSD) of the iEEG signal between 0 and 125 Hz using the Welch method (2 s-segments, 12.4% overlap).

**Fitting Oscillations and 1/f (FOOF) Method.** PSDs for each channel across conditions were analyzed using the FOOOF method (23) which parameterizes aperiodic and periodic features of the power spectrum allowing us to determine whether FA meditation induces true oscillatory changes in neural activity or impacts other neurophysiological processes. Consistent with prior work leveraging the FOOOF method to assess human electrophysiological data, we visually inspected each PSD to determine the appropriate method of aperiodic fitting (linear versus nonlinear). Across most channels ( $n = 26$ ), PSDs depicted a bend in higher frequencies ( $>40$  Hz), therefore spectral parameterization with FOOOF was performed using a knee to appropriately capture these power spectra's nonlinear dynamics (Fig. 2B). This was consistent with existing human electrophysiology literature, especially when evaluating higher frequency domains ( $>40$  Hz). In one channel, a bend was not observed in the PSD. Spectral parameterization for this channel was performed without a knee. Using fitted exponent and knee parameters for each channel, we calculated the knee frequency to evaluate group differences. The knee frequency reflects the frequency in which the aperiodic slope of the PSD changes. Further, peak width was restricted to 1 to 8 Hz to minimize overfitting. Model fit was evaluated according to R-squared and error metrics (Amygdala: median  $R^2$ (median error) = baseline (0.99(0.03)), meditation (0.99(0.04)); Hippocampus: baseline (0.99(0.03)), meditation (0.99(0.03))). R-squared for both regions was in accordance with existing literature (68) and not significantly different between conditions suggesting good fit for both the amygdala ( $P > 0.05$ , two-sided paired-samples Wilcoxon signed rank test) and hippocampus ( $P > 0.05$ , two-sided paired-samples Wilcoxon signed rank test).

Using the FOOOF method, we fit the aperiodic (offset, knee, exponent) and periodic (power, bandwidth, center frequency) components of each iEEG channel's power spectrum between 2 and 55 Hz for each condition (Fig. 2B). This allowed us to separate true oscillatory features of the PSD versus background (1/f) neural activity, characterized by the aperiodic components (69). The aperiodic offset, or broadband intercept, reflects the up/down translation of the spectrum while the aperiodic exponent reflects the overall curve of the aperiodic component with a smaller exponent reflecting a shallower power spectrum (Fig. 2B). Oscillations are reflected as narrowband peaks in power above the aperiodic component of the PSD. Parameterizing both the periodic and aperiodic components of the PSD allows us to compare differences in the presence/absence of oscillations at individual frequency bands between regions and conditions, as well as the periodic features of those oscillations while accounting for the background 1/f aperiodic profile which reflects other physiological processes. Periodic components of the power spectra refer to activity with a characteristic frequency. Of interest for the present study is frequency-specific power, which quantifies the amount of energy contained in the iEEG signal at a particular frequency band. Aperiodic components of the power spectra refer to recorded activity with no characteristic frequency. We assessed LKM-associated differences in aperiodic offset, which measures the overall up/down translation of the power spectra, exponent, which reflects the slope of the aperiodic component of the power spectra, and the knee frequency, which quantifies the aperiodic component's "bend" or transition point wherein the dominant characteristics of the neural signal change (Fig. 2B; 23). For each channel, we estimated power in putative frequency bands by taking the average power of peaks above the aperiodic component falling within a priori designated ranges according to their center frequency ( $\delta = 2-4$  Hz,  $\theta = 4-8$  Hz,  $\alpha = 8-13$  Hz,  $\beta = 13-30$  Hz,  $\gamma = 30-55$  Hz).

**Quantifying Subject-Level Beta and Gamma Power Modulations.** Data from each condition (baseline and LKM) were segmented into 1-s non-overlapping epochs. Time-frequency representations of power were computed for each epoch using Morlet wavelet convolution. For each frequency (in a logarithmically spaced range between 1 and 60 Hz), the number of cycles used in the wavelet transformation was defined as half of the frequency value. We extracted power estimates

corresponding to the beta (13 to 30 Hz) and gamma (30 to 55 Hz) frequency range separately for each frequency band. Power values within each range were averaged across the frequency dimension for each epoch and channel, providing a measure of broadband beta and gamma power, respectively, for further analysis. To assess changes in beta power during meditation relative to baseline, z-scores were computed for the LKM epochs. First, the mean and SD of baseline power values were calculated across epochs and time points for each channel and used to z-score each LKM epoch across channels for each subject, yielding normalized values that reflect relative deviations from baseline (Fig. 6). For each subject, the median z-scored beta power was computed across all epochs and channels.

**eBOSC Method.** To assess FA meditation-induced temporal differences in oscillatory activity, we estimated the duration of oscillations by applying the eBOSC method (24, 70). By calculating both the strength (i.e., amplitude) and duration of a given oscillation, eBOSC provides a comprehensive characterization of oscillatory events. eBOSC allowed us to estimate the duration of oscillations by identifying significant oscillations that surpass a statistical power threshold, extracting the number of detected cycles in each significant oscillation, and converting the number of detected cycles to duration in a frequency-specific manner. eBOSC first performs time-frequency decomposition on continuous data. The resulting power spectra are fit linearly using robust regression to estimate the relationship between  $\log(\text{frequency})$  and  $\log(\text{power})$ . A power threshold for each frequency was set at the 95% of a  $\chi^2$ -distribution of power values centered around the fitted estimate of background power at a given frequency based on the linear model fit. This establishes a statistical power threshold for determining a significant oscillation at a given frequency. Using the derived power threshold, oscillations and their associated time intervals were extracted. The duration threshold was set to zero, allowing us to compare both transient and sustained oscillatory episodes. The proportion of time spent oscillating at each frequency is calculated by summing detected time intervals and normalizing by total duration of a given iEEG recording.

#### Statistics.

**Data quality checks.** We used a nonparametric Pearson's chi-square goodness-of-fit test to determine whether there was a significant difference in the proportion of data within each condition following preprocessing. We used a nonparametric Wilcoxon rank-sum test to check whether FOOOF model fit ( $R^2$ ) differed significantly between conditions.

**Hypothesis testing.** We used a nonparametric Fisher's exact test to assess whether a nonrandom association exists between experimental condition (baseline versus meditation) and categorical variables (presence versus absence of an oscillation within a given frequency band). To assess significant differences between conditions for linear variables (oscillatory power and duration), we used nonparametric Wilcoxon rank-sum tests. One-sided Wilcoxon rank-sum tests were implemented where applicable based on empirical literature regarding meditation-induced modulation of  $\beta$  and  $\gamma$  oscillations (3, 16, 17).

**Data, Materials, and Software Availability.** Anonymized data from participants who consented to data sharing are available upon request with the approval of NeuroPace. Analysis scripts can be found at the following GitHub repository: [https://github.com/christinamaher/iEEG\\_LKM](https://github.com/christinamaher/iEEG_LKM) (71).

**ACKNOWLEDGMENTS.** We thank Jill Gregory, Master of Fine Arts, Certified Medical Interpreter, Associate Director of Instructional Technology at the Icahn School of Medicine at Mount Sinai, for illustrating Fig. 1A. We would like to thank the patient and research and surgical staff at the recording site for their support and dedication. This project was supported by a Nash Family Research Scholars Award to J.Y., A.W., H.S.M., and F.P.

1. R. Chambers, E. Gullone, N. B. Allen, Mindful emotion regulation: An integrative review. *Clin. Psychol. Rev.* **29**, 560-572 (2009).
2. A. Lutz, J. Brefczynski-Lewis, T. Johnstone, R. J. Davidson, Regulation of the neural circuitry of emotion by compassion meditation: Effects of meditative expertise. *PLoS One* **3**, e1897 (2008).
3. A. Lutz, L. L. Greischar, N. B. Rawlings, M. Ricard, R. J. Davidson, Long-term meditators self-induce high-amplitude gamma synchrony during mental practice. *Proc. Natl. Acad. Sci. U.S.A.* **101**, 16369-16373 (2004).
4. A. Lutz, H. A. Slagter, J. D. Dunne, R. J. Davidson, Attention regulation and monitoring in meditation. *Trends Cogn. Sci.* **12**, 163-169 (2008).

5. J. A. Brefczynski-Lewis *et al.*, Neural correlates of attentional expertise in long-term meditation practitioners. *Proc. Natl. Acad. Sci. U.S.A.* **104**, 11483-11488 (2007).
6. S. L. Shapiro, G. E. Schwartz, G. Bonner, Effects of mindfulness-based stress reduction on medical and premedical students. *J. Behav. Med.* **21**, 581-599 (1998).
7. J. Wielgosz *et al.*, Mindfulness meditation and psychopathology. *Annu. Rev. Clin. Psychol.* **15**, 285-316 (2019).
8. M. Boccia, L. Piccardi, P. Guariglia, The meditative mind: A comprehensive meta-analysis of MRI studies. *Biomed Res. Int.* **2015**, 419808 (2015).
9. C. Kaur, P. Singh, EEG derived neuronal dynamics during meditation: Progress and challenges. *Adv. Prev. Med.* **2015**, 614723 (2015).

10. C. J. Dahl, A. Lutz, R. J. Davidson, Reconstructing and deconstructing the self: Cognitive mechanisms in meditation practice. *Trends Cogn. Sci.* **19**, 515–523 (2015).
11. C. Craboszcz *et al.*, Increased gamma brainwave amplitude compared to control in three different meditation traditions. *PLoS One* **12**, e0170647 (2017).
12. J. Petrovic *et al.*, The effects of loving-kindness interventions on positive and negative mental health outcomes: A systematic review and meta-analysis. *Clin. Psychol. Rev.* **110**, 102433 (2024).
13. G. Desbordes *et al.*, Effects of mindful-attention and compassion meditation training on amygdala response to emotional stimuli in an ordinary, non-meditative state. *Front. Hum. Neurosci.* **6**, 292 (2012).
14. M.-K. Leung *et al.*, Increased gray matter volume in the right angular and posterior parahippocampal gyri in loving-kindness meditators. *Soc. Cogn. Affect. Neurosci.* **8**, 34–39 (2013).
15. J. Lachaux *et al.*, Relationship between task-related gamma oscillations and BOLD signal: New insights from combined fMRI and intracranial EEG. *Hum. Brain Mapp.* **28**, 1368–1375 (2007).
16. M. Irmischer *et al.*, Controlling the temporal structure of brain oscillations by focused attention meditation. *Hum. Brain Mapp.* **39**, 1825–1838 (2018).
17. M. Irmischer *et al.*, Strong long-range temporal correlations of beta/gamma oscillations are associated with poor sustained visual attention performance. *Eur. J. Neurosci.* **48**, 2674–2683 (2018).
18. E. K. Miller, T. J. Buschman, Cortical circuits for the control of attention. *Curr. Opin. Neurobiol.* **23**, 216–222 (2013).
19. T. J. Buschman, E. K. Miller, Top-down versus bottom-up control of attention in the prefrontal and posterior parietal cortices. *Science* **315**, 1860–1862 (2007).
20. S. Alagapan *et al.*, Cingulate dynamics track depression recovery with deep brain stimulation. *Nature* **622**, 130–138 (2023).
21. O. G. Sani *et al.*, Mood variations decoded from multi-site intracranial human brain activity. *Nat. Biotechnol.* **36**, 954–961 (2018).
22. J. J. Young *et al.*, Elevated phase amplitude coupling as a depression biomarker in epilepsy. *Epilepsy Behav.* **152**, 109659 (2024).
23. T. Donoghue *et al.*, Parameterizing neural power spectra into periodic and aperiodic components. *Nat. Neurosci.* **23**, 1655–1665 (2020).
24. J. Q. Kosciessa *et al.*, Single-trial characterization of neural rhythms: Potential and challenges. *Neuroimage* **206**, 116331 (2020).
25. N. von Ellenrieder *et al.*, Electrode and brain modeling in stereo-EEG. *Clin. Neurophysiol.* **123**, 1745–1754 (2012).
26. S. Arcot Desai *et al.*, Quantitative electrocorticographic biomarkers of clinical outcomes in mesial temporal lobe epileptic patients treated with the RNS® system. *Clin. Neurophysiol.* **130**, 1364–1374 (2019).
27. S. E. Qasim *et al.*, Neuronal activity in the human amygdala and hippocampus enhances emotional memory encoding. *Nat. Hum. Behav.* **7**, 754–764 (2023).
28. J. Parvizi, S. Kastner, Human intracranial EEG: Promises and limitations. *Nat. Neurosci.* **21**, 474–483 (2018).
29. S. L. L. Maoz *et al.*, Dynamic neural representations of memory and space during human ambulatory navigation. *Nat. Commun.* **14**, 6643 (2023).
30. Z. M. Aghajani *et al.*, Theta oscillations in the human medial temporal lobe during real-world ambulatory movement. *Curr. Biol.* **27**, 3743–3751.e3 (2017).
31. C. B. Josephson *et al.*, Association of depression and treated depression with epilepsy and seizure outcomes: A multicohort analysis. *JAMA Neurol.* **74**, 533–539 (2017).
32. I. Saez *et al.*, Encoding of multiple reward-related computations in transient and sustained high-frequency activity in human OFC. *Curr. Biol.* **28**, 2889–2899.e3 (2018).
33. L. Marcuse, M. Fields, J. Yoo, *Rowan's Primer of EEG* (Elsevier, ed. 2, 2015).
34. T. A. Whitten *et al.*, A better oscillation detection method robustly extracts EEG rhythms across brain state changes: The human alpha rhythm as a test case. *Neuroimage* **54**, 860–874 (2011).
35. A. Wynne, *The Origin of Buddhist Meditation* (Routledge, 2007).
36. A. Manna *et al.*, Neural correlates of focused attention and cognitive monitoring in meditation. *Brain Res. Bull.* **82**, 46–56 (2010).
37. M. Engström *et al.*, Functional magnetic resonance imaging of hippocampal activation during silent mantra meditation. *J. Altern. Complement. Med.* **16**, 1253–1258 (2010).
38. B. L. Fredrickson *et al.*, Open hearts build lives: Positive emotions, induced through loving-kindness meditation, build consequential personal resources. *J. Pers. Soc. Psychol.* **95**, 1045–1062 (2008).
39. F. Ferrarelli *et al.*, Experienced mindfulness meditators exhibit higher parietal-occipital EEG gamma activity during NREM sleep. *PLoS One* **8**, e73417 (2013).
40. K. A. Garrison *et al.*, Meditation leads to reduced default mode network activity beyond an active task. *Cogn. Affect. Behav. Neurosci.* **15**, 712–720 (2015).
41. D. Roberts-Wolfe *et al.*, Mindfulness training alters emotional memory recall compared to active controls: Support for an emotional information processing model of mindfulness. *Front. Hum. Neurosci.* **6**, 15 (2012).
42. C. C. van Schie *et al.*, When I relive a positive me: Vivid autobiographical memories facilitate autonoetic brain activation and enhance mood. *Hum. Brain Mapp.* **40**, 4859–4871 (2019).
43. C. Poskanzer, M. Aly, Switching between external and internal attention in hippocampal networks. *J. Neurosci.* **43**, 6538–6552 (2023).
44. Y. Zhu *et al.*, Emotion regulation of hippocampus using real-time fMRI neurofeedback in healthy human. *Front. Hum. Neurosci.* **13**, 242 (2019).
45. M. F. Carr *et al.*, Hippocampal replay in the awake state: A potential substrate for memory consolidation and retrieval. *Nat. Neurosci.* **14**, 147–153 (2011).
46. B. J. Wilting *et al.*, The hippocampus plays a selective role in the retrieval of detailed context memories. *Curr. Biol.* **20**, 1336–1344 (2010).
47. R. H. A. H. Jacobs *et al.*, The amygdala, top-down effects, and selective attention to features. *Neurosci. Biobehav. Rev.* **36**, 2069–2084 (2012).
48. C. Klinge *et al.*, Increased amygdala activation to emotional auditory stimuli in the blind. *Brain* **133**, 1729–1736 (2010).
49. C. J. Peck, C. D. Salzman, Amygdala neural activity reflects spatial attention towards stimuli promising reward or threatening punishment. *Elife* **3**, e04478 (2014).
50. L. Pessoa, R. Adolphs, Emotion processing and the amygdala: From a 'low road' to 'many roads' of evaluating biological significance. *Nat. Rev. Neurosci.* **11**, 773–783 (2010).
51. M. Lundqvist *et al.*, Beta: Bursts of cognition. *Trends Cogn. Sci.* **28**, 662–676 (2024).
52. M. Bocchio *et al.*, Synaptic plasticity, engrams, and network oscillations in amygdala circuits for storage and retrieval of emotional memories. *Neuron* **94**, 731–743 (2017).
53. Y. Li *et al.*, Beta oscillations in major depression—Signalling a new cortical circuit for central executive function. *Sci. Rep.* **7**, 18021 (2017).
54. S. L. Brincat *et al.*, Interhemispheric transfer of working memories. *Neuron* **109**, 1055–1066.e4 (2021).
55. S. Kim *et al.*, Alteration of cortical functional networks in mood disorders with resting-state electroencephalography. *Sci. Rep.* **12**, 5920 (2022).
56. J. N. Sanes, J. P. Donoghue, Oscillations in local field potentials of the primate motor cortex during voluntary movement. *Proc. Natl. Acad. Sci. U.S.A.* **90**, 4470–4474 (1993).
57. F. Torrecillos *et al.*, Distinct modulations in sensorimotor postmovement and foreperiod  $\beta$ -band activities related to error salience processing and sensorimotor adaptation. *J. Neurosci.* **35**, 12753–12765 (2015).
58. P. Khanna, J. M. Carmena, Beta band oscillations in motor cortex reflect neural population signals that delay movement onset. *Elife* **6**, e24573 (2017).
59. H. T. Darch *et al.*, Pre-movement changes in sensorimotor beta oscillations predict motor adaptation drive. *Sci. Rep.* **10**, 17946 (2020).
60. S. Meisenhelter *et al.*, Cognitive tasks and human ambulatory electrocorticography using the RNS system. *J. Neurosci. Methods* **311**, 408–417 (2019).
61. V. R. Rao *et al.*, Chronic ambulatory electrocorticography from human speech cortex. *Neuroimage* **153**, 273–282 (2017).
62. E. L. Rich, J. D. Wallis, Spatiotemporal dynamics of information encoding revealed in orbitofrontal high-gamma. *Nat. Commun.* **8**, 1139 (2017).
63. P. Fries, Neuronal gamma-band synchronization as a fundamental process in cortical computation. *Annu. Rev. Neurosci.* **32**, 209–224 (2009).
64. P. Fries *et al.*, The gamma cycle. *Trends Neurosci.* **30**, 309–316 (2007).
65. M. Seeber *et al.*, Human neural dynamics of real-world and imagined navigation. bioRxiv [Preprint] (2024). <https://doi.org/10.1101/2024.05.23.595237> (Accessed 23 May 2024).
66. C. J. May *et al.*, Short-term training in loving-kindness meditation produces a state, but not a trait, alteration of attention. *Mindfulness* **2**, 143–153 (2011).
67. Y. C. Leong *et al.*, Dynamic interaction between reinforcement learning and attention in multidimensional environments. *Neuron* **93**, 451–463 (2017).
68. H. McGrath *et al.*, High-resolution cortical parcellation based on conserved brain landmarks for localization of multimodal data to the nearest centimeter. *Sci. Rep.* **12**, 18778 (2022).
69. M. Kopčanová *et al.*, Resting-state EEG signatures of Alzheimer's disease are driven by periodic but not aperiodic changes. *Neurobiol. Dis.* **190**, 106380 (2024).
70. L. Hu *et al.*, Single-trial time-frequency analysis of electrocortical signals: Baseline correction and beyond. *Neuroimage* **84**, 876–887 (2014).
71. C. Maher, iEEG\_LKM. GitHub. [https://github.com/christinamaher/iEEG\\_LKM](https://github.com/christinamaher/iEEG_LKM). Accessed 10 January 2025.